Pharmaceutical Research, Vol. 24, No. 9, September 2007 (© 2007)
DOI: 10.1007/s11095-007-9292-6

Research Paper

Insulin Self-association: Effects on Lung Disposition Kinetics in the Airways of the Isolated Perfused Rat Lung (IPRL)

Yinuo Pang,[1,2] Masahiro Sakagami,[1,3] and Peter R. Byron[1]

Received November 7, 2006; accepted March 8, 2007; published online May 3, 2007

Purpose. To characterize the kinetic dependence of pulmonary absorption and metabolism of insulin and lispro on the magnitude of their hexameric association.
Methods. Hexamer content by weight percent (%Hex) in various insulin-zinc and lispro-zinc solutions were determined by quantitative centrifugal ultrafiltration and zinc titration with terpyridine (QCUF-ZTT). Each of the solutions (0.1 ml) was then administered into the airways of the IPRL of normal and experimental diabetic animals. Rate constants were determined for lung absorption (k_a) and non-absorptive loss (k_{nal}; comprising mucociliary clearance and metabolism).
Results. %Hex in administered solutions ranged from 3.3 to 94.4%. Data analysis showed excellent correlations between the values for k_a or k_{nal} and %Hex, irrespective of insulin type, concentration, solution pH or ionic strength. The values for k_a decreased ($0.22 \rightarrow 0.05\ h^{-1}$) with increasing %Hex, as did values for k_{nal}. At %Hex in administered solutions $\geq 50\%$, values for k_{nal} approached estimates for the rate constant for mucociliary clearance, implying that lung metabolism occurred primarily with monomeric insulin. There were no differences in insulin disposition kinetics between lungs taken from experimental diabetic and sham-control animals.
Conclusions. The kinetics of pulmonary insulin disposition depended on the magnitude of molecular self-association. Dissociated forms of insulin (dimers or monomers) in the dosing solution showed higher rates than hexamers for both lung absorption and metabolism.

KEY WORDS: inhalation; insulin; kinetics; lung; self-association.

INTRODUCTION

Insulin is a unique polypeptide hormone exhibiting complex self-association properties during its action as a physiological regulator as well as in aqueous solutions (1,2). It exists as an equilibrium mixture of monomers, dimers, tetramers and hexamers, depending on insulin concentration, solution pH and ionic strength, and the presence of certain metal ions and phenolic analogues (1,2). Among these options, formulation stability can be achieved with insulin hexamers in complexes with two zinc ions in the structure, which is the form in which the hormone is stored in the pancreatic β cells; secreted and circulating insulin primarily exists as monomers (1,2). Ironically however, this hexameric association of insulin in pharmaceutical formulations is known to result in a delayed onset of glucose reduction following subcutaneous injection, since rapid penetration across capillary membranes appears to occur only after dissociation into dimers and/or monomers (1–3). This has led to the successful development of genetically modified "monomeric" insulin analogues, e.g., insulin lispro (Humalog®) and aspart (Novolog®), as rapid-acting subcutaneous formulations for postprandial glycemic control in diabetes; these analogues associate to form hexamers at higher concentrations than regular and endogenous insulin (2,4,5).

The desire to mimic normal endogenous postprandial glycemic profiles noninvasively in diabetic subjects has triggered the development of inhaled insulin. The lung's high solute permeability, large surface area, extensive vasculature and lowered proteolytic activity in its alveolar regions have all contributed to this venture (6,7). Although only regular insulin has been used so far, this route of administration has accomplished faster onset and comparable duration of action in humans, even when compared to subcutaneous injection of rapid-acting insulin, lispro (8). Meanwhile, the impact of insulin's hexameric association on lung disposition and

[1] Department of Pharmaceutics, School of Pharmacy, Virginia Commonwealth University, 410 N. 12th Street, P.O. Box 980533, Richmond, Virginia 23298-0533, USA.
[2] *Present Address*: Schering-Plough Biopharma, Palo Alto, California, USA.
[3] To whom correspondence should be addressed. (e-mail: msakagam@vcu.edu)

ABBREVIATIONS: BSA, bovine serum albumin; CBS, citrate-buffered saline; CD, circular dichroism; COD, coefficient of determination; ELISA, enzyme-linked immunosorbent assay; %Hex, percent of hexamers by weight; IPRL, isolated perfused rat lung; IU, International Unit; LLF, lung lining fluid; MSC, model selection criterion; NIH, National Institute of Health; PBS, phosphate-buffered saline; QCUF–ZTT, quantitative centrifugal ultrafiltration and zinc titration with terpyridine; %RSD, percent of relative standard deviation; SD, standard deviation; SE, standard error; STZ, streptozotocin; $t_{1/2}$, apparent half-life; USP, United States Pharmacopeia; UV, ultraviolet; VCU, Virginia Commonwealth University; μ, ionic strength; [θ], mean residue molar ellipticity.

glucose reduction profiles following inhalation has been mentioned in the patent literature (9), yet not been studied systematically due to an uncertainty associated with the magnitude and/or kinetics of insulin's self-association on the surface of the lung. Indeed, we postulated that insulin dosing to a limited volume of lung lining fluid (LLF) potentially creates hexamer-rich compositions on the lung surface. This phenomenon could explain results from our previous study with the isolated perfused rat lung (IPRL), where airway administration of regular insulin at 15 IU/ml (≈0.6 mg/ml) yielded much lower absorption from the lung, compared to that at 3 IU/ml (≈0.12 mg/ml; 10). If so, like subcutaneous injection (1–3), lung disposition kinetics of pulmonary insulin would be affected by self-association and the extent of hexamer formation at the absorption site.

The present study continued to employ our well-controlled IPRL preparation with lungs derived from normal and experimental diabetic animals. The objective of the study was to derive the dependence of insulin's kinetic descriptors in the lung (i.e., rate constants) following pulmonary administration upon the magnitude of hexameric self-association in the dosing solutions. Insulin-zinc (Ins-Zn) and lispro-zinc (Lispro-Zn) were prepared at various concentrations in solution formulations, and the amounts of insulin present as hexamer were determined by a new quantitative technique. Then, each of these solutions was administered into the airways of the IPRL, and absorption data were analyzed with a previously developed kinetic model (Fig. 1; 10), deriving the rate constants for lung absorption (k_a) and non-absorptive loss (k_{nal}).

MATERIALS AND METHODS

Chemicals

Recombinant human insulin-zinc (Ins-Zn; 28.7 USP IU/mg) was purchased from Sigma-Aldrich (St. Louis, MO), whereas human insulin lispro-zinc (Lispro-Zn; 28.9 USP IU/mg) was a generous gift from Eli Lilly and Company (Greenfield, IN).

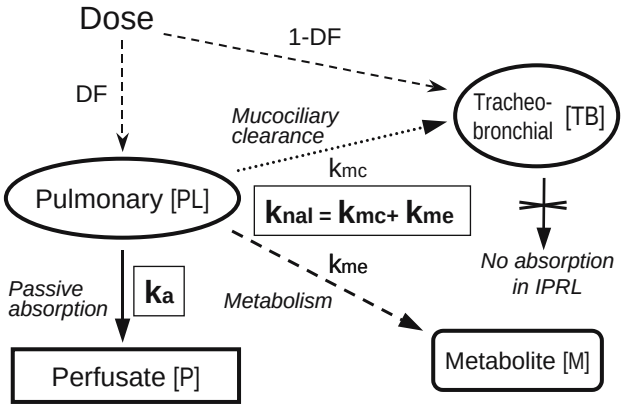

Fig. 1. The kinetic scheme that describes insulin disposition in the airways of the isolated perfused rat lung (IPRL; 10). Insulin absorption from the tracheobronchial region is absent due to the severance of the bronchial circulation. Key: DF: initial average distribution fraction to the perfused pulmonary regions following an 0.1 ml coarse spray administration (0.91; 10,18); k_a: apparent first-order rate constant for passive absorption from PL; k_{nal}: apparent first-order rate constant for non-absorptive loss from PL, comprised of k_{mc} and k_{me}, the first-order rate constants for mucociliary clearance and metabolism, respectively.

Both crystalline solids contained 0.5% of zinc by weight, according to the suppliers. Zinc chloride ($ZnCl_2$; ACS Reagent), bovine serum albumin (BSA; fraction V; >98%), 2,2′:6′,2″-terpyridine (Terpy; 98%) and streptozotocin (STZ; 98%) were obtained from Sigma-Aldrich (St. Louis, MO). Other chemicals used to prepare Krebs–Henseleit buffer (pH 7.4), 50 and 5 mM phosphate-buffered saline (PBS; pH 7.4 and 3.0, respectively), 20 mM citrate-buffered saline (CBS; pH 4.5) and 0.1 M HCl, i.e., D-glucose, KCl, $MgSO_4{\cdot}7H_2O$, $NaHCO_3$, $CaCl_2{\cdot}2H_2O$, NaCl, KH_2PO_4, $NaH_2PO_4{\cdot}2H_2O$, $Na_2HPO_4{\cdot}7H_2O$, $HOC(COOH)(CH_2COOH)_2{\cdot}H_2O$, $HOC(COONa)(CH_2COONa)_2{\cdot}2H_2O$ and HCl, were all purchased from Fisher Scientific (Pittsburgh, PA). These buffer solutions were prepared, as described previously (10–12).

Insulin Solution Preparation

Ins-Zn and Lispro-Zn powders were weighed and dissolved in 0.1 ml of 0.1 M HCl, followed by appropriate dilution with either 50 mM PBS at pH 7.4 or 5 mM PBS at pH 3.0 (ionic strength, μ = 0.28 and 0.16 M, respectively), in order to prepare 0.025, 0.05, 0.1, 0.15, 0.2, 0.3, 0.5 and 1.0 mg/ml of insulin and lispro solutions. Each solution was prepared in a silicone-coated tube (VACUTAINER®; Becton Dickinson and Company, Franklin Lakes, NJ) and used as a dosing solution in the IPRL following characterization of the degree of hexamer formation (%Hex).

Characterization of Hexameric Association of Insulin and Lispro in Solution

Quantitative Centrifugal Ultrafiltration and Zinc Titration with Terpyridine (QCUF-ZTT)

The magnitude of hexameric association of insulin and lispro in each of the buffer solutions was determined by the QCUF–ZTT technique described below. The method employed centrifugal filter units (Ultrafree®-MC, 10 kDa molecular weight cut-off, Millipore Corporation, Billerica, MA) and zinc titration with a chromophoric chelator, Terpy, that forms a complex of $(Terpy)_2Zn$ in the presence of zinc (13,14). Ins-Zn or Lispro-Zn solutions at various concentrations (0.025–1.0 mg/ml) in 50 mM PBS at pH 7.4 or 5 mM PBS at pH 3.0 were ultrafiltered in the filter units by centrifugation at 11,752 g (12,000 rpm; Eppendorf Centrifuge 5415C, Brinkman Instruments Inc., Westbury, NY) for 30 min. This enabled theoretical separation of "zinc bound to insulin hexamers" retained in the filter unit from "unbound zinc" collected in the filtrate, due to their apparent molecular weight differences (hexamers are ~36 kDa, while dimers and monomers of insulin are inefficient complex agents for Zn^{2+}; 1,2,13,14). Subsequently, both the original and the filtrate solutions were subjected to chelation with an excess of 350 μM Terpy for 90 min at room temperature to complete the formation of the $(Terpy)_2Zn$ complex (13,14). This chelating condition was selected to determine zinc content in solution, based on the literature reporting rapid and complete complex formation, when molar Terpy concentrations exceeded 20-fold of zinc concentration ([Zn]) whether the original source of Zn^{2+} was free or bound to insulin hexamers (13,14). Thus, "total" and "unbound" zinc concentrations ($[Zn]_{total}$ and

$[Zn]_{unbound}$) were determined from the original and the filtrate solutions, respectively by UV absorbance (UV2401, Shimadzu Corporation, Kyoto, Japan) at 333 nm using 350 μM Terpy as reference solution. Standard calibration curves for $[Zn]_{total}$ and $[Zn]_{unbound}$ were constructed for each assay by subjecting $ZnCl_2$-spiked samples, both with and without insulin, to the assay described above. This revealed (a) that Terpy removed all available zinc from insulin in solution, (b) that predictable mean losses of unbound zinc occurred during centrifugation were 23% (95%CI = 18–27%) and (c) that linear calibration curves resulted, following correction for filtration-induced losses, in $R^2 \geq 0.999$ over the range of initial [Zn] = 0.4–15 μM with a precision or relative standard deviation, %RSD ≤ 10%. When the assay was used to estimate % fractions of Zn relative to insulin by weight in the original solutions of Ins-Zn and Lispro-Zn, values were determined to be 0.51 ± 0.12 and 0.48 ± 0.04% (mean ± SD, $n = 13$), respectively, consistent with the suppliers' claim and thus, titration accuracy. Percentage insulin present in solution in the form of hexamers (%Hex) was estimated in each dosing solution containing known concentrations of insulin, by determining the 333 nm absorbance of the solution itself and that of the filtrate after complexation with 350 μM Terpy. Bound zinc ($[Zn]_{bound}$) was determined by difference between the results for [Zn] in the dosing solution and the filtrate:

$$[Zn]_{bound} = [Zn]_{total} - [Zn]_{unbound} \quad (1)$$

Subsequently, %Hex was determined from $[Zn]_{bound}$, assuming the stoichiometry of $(insulin)_6Zn_2$ (1–4), using Eq. 2:

$$\%Hex = 100 \times \left([Zn]_{bound} \times 3\right)/[Ins] \quad (2)$$

where [Ins] is the known molar concentration expressed as monomers in each solution.

Far and Near UV Circular Dichroic (CD) Spectrometry

In order to validate QCUF-ZTT further, semi-quantitative characterization of hexameric association was carried out using far and near UV CD spectra of Ins-Zn solutions at various concentrations (0.025–1.0 mg/ml) in 50 mM PBS at pH 7.4. Ins-Zn solutions were prepared, as described above. Their CD spectra in the far (200–260 nm) and near (250–330 nm) UV ranges were acquired in triplicate at room temperature (RSM CD spectrophotometer, OLIS Inc., Bogart, GA). Each of the CD spectra was subjected to baseline subtraction using PBS samples containing no Ins–Zn. While the data were recorded as ellipticity (θ; in mdeg), mean residue molar ellipticity ($[\theta]$; in deg·cm^2/(dmol·residue)) was calculated using Eq. 3:

$$[\theta] = (\theta \cdot MW)/(C \cdot L \cdot n \cdot 10) \quad (3)$$

where MW is the human insulin molecular weight [5,808 g/mol], C is the insulin concentration [g/l], L is the optical cell path length [cm], and n is the number of amino acid residues per molecule [51 residues for human insulin].

Animals

Sprague–Dawley rats (male; specific-pathogen-free) weighing 300–325 g (Hilltop Laboratory Animals Inc., Scottsdale, PA) were housed in rooms controlled between 20–25°C and 40–70% relative humidity with dark–light cycling every 12 h. The animals had free access to food and water during acclimation prior to experimentation. In animals where STZ-induced diabetes was developed, smaller rats weighing 200–225 g were treated according to the protocol developed by Chandrashekar *et al.* (15). Briefly, STZ dissolved in 20 mM CBS (pH 4.5) was injected intraperitoneally at a dose of 40 mg/kg body weight once daily for the first 3 days. These animals were housed under the conditions described above and considered diabetic when their fasted blood glucose levels exceeded 250 mg/dl 2 weeks following STZ injections; at this time, their body weights had increased to a range suitable for the IPRL experiments (Table I). CBS injections (without STZ) were carried out under an identical protocol to provide matched sham-control animals. All of the experiments and protocols employed in this study adhered to the NIH Principles of Laboratory Care and were approved by the Institutional Animal Care and Use Committee of Virginia Commonwealth University.

Insulin Disposition in the Isolated Perfused Rat Lung (IPRL)

The IPRL preparation and the dosing method, forced solution instillation, was performed, as described in detail previously (10,16–18). Briefly, a rat lung was surgically removed under pentobarbital anesthesia and housed horizontally in an artificial thorax maintained at 37°C. Krebs–Henseleit buffer containing 4% (w/v) BSA was used as perfusate and re-circulated through the pulmonary circulation at a constant flow rate of 15 ml/min. Ins-Zn or Lispro-Zn solutions at various concentrations (0.025–1.0 mg/ml) in 50 mM PBS at pH 7.4 or 5 mM PBS at pH 3.0 were prepared, as described above. A metal dosing cartridge containing 0.1 ml of these solutions was inserted into the trachea via an exteriorized cannula port, so that the cartridge tip projected 0.5 mm beyond the cannula terminus in the trachea. The dosing solution was then propelled into the airways as a coarse spray by a single actuation of a propellant-only metered dose inhaler, thereby completing the forced solution instillation (10,16–18). The cartridge was removed immediately, and the lung allowed deflating to a volume defined by the maintenance of a slight hypobaric condition (2–3 cmH_2O below atmospheric) in the artificial thorax. Our previous studies (10,18) have thoroughly validated that this dosing method, with 0.1 ml solution, enabled an averaged 91% of the expelled dose to be delivered into the perfused pulmonary lobar regions, irrespective of solute and concentration. The IPRL preparation was considered to be viable for ≥ 1 h, evidenced by the absence of pulmonary edema and any notable discontinuity in the administered solute's airway-to-perfusate transfer vs. time profile, as in our previous studies (10,16–18).

Insulin and lispro absorption were characterized by their appearance in perfusate over time. Perfusate samples (0.5 ml) were taken from the reservoir at different time intervals following instillation, and the volume replaced with fresh perfusate post-sampling. Insulin and lispro concentrations in the perfusate samples were determined by validated enzyme-linked immunosorbent assays (ELISA; Insulin and Iso-Insulin EIA, respectively; ALPCO, Windham, NH) using the manufacture's protocol. It should be noted that, across doses

Table I. Derived IPRL Disposition Parameters for Insulin in Experimental Diabetes and Matched Sham-controls

Animal	Body weight[a] [g]	Blood glucose[a] [mg/dl]	Rate constant[b] [h^{-1}]		MSC; COD[c]
			k_a	k_{nal}	
Sham-control	346 ± 18	98 ± 12	0.10 ± 0.02	1.43 ± 0.22	5.66; 0.997
STZ-induced	294 ± 36	274 ± 20	0.10 ± 0.02	1.76 ± 0.34	4.94; 0.996

First-order absorption (k_a) and non-absorptive loss (k_{nal}) following 0.1 ml doses of 0.1 mg/ml Ins-Zn in 50 mM PBS (pH 7.4) into lungs prepared from streptozotocin (STZ)-induced experimental diabetic and matched sham-control animals.
[a] Body weight and blood glucose data were taken at 2 weeks following intraperitoneal injections of citrate-buffered saline (CBS) or STZ in CBS, respectively; each of the data represents mean ± standard deviation (SD) with $n = 4$.
[b] Rate constant data represent mean ± 95% confidence interval (95%CI); these were derived by curve-fitting the mean IPRL profiles with $n = 4$ to the model shown in Fig. 1.
[c] MSC (model selection criterion) and COD (coefficient of determination) were calculated by Scientist™.

tested in this study, their concentrations were ≤0.02 μg/ml where only monomer can exist (1–3). Both kits were successfully validated in-house for insulin and lispro quantification in perfusate within- and between-lots with precision and accuracy ≤15%. The concentration was multiplied by perfusate volume and converted to mass absorbed into the perfusate. Cumulative % of administered dose transferred to perfusate was calculated at each sampling time, from the quotient of absorbed mass divided by the administered dose.

Estimation of Rate Constants from the IPRL Profiles

The kinetic model shown as Fig. 1 was developed and used in our previous study (10) in order to describe lung disposition of insulin and lispro following administration to the airways of the IPRL. It assumed two lung compartments, pulmonary lobar (PL) and tracheobronchial (TB) regions spatially defined by their vascular beds (the pulmonary and bronchial circulations, respectively). Following 0.1 ml solution instillation, an initial mean distribution fraction (DF) of 0.91 reached the PL region (10,18), from which three simultaneous parallel kinetic processes (absorption, mucociliary clearance and metabolism) were assumed to take place, described by apparent first-order rate constants, k_a, k_{mc} and k_{me}, respectively. No absorption was assumed possible from the TB region of the IPRL, due to surgical severance of the bronchial circulation during preparation; this was validated previously, while being apparently valid to predict *in vivo* behavior for large molecular weight solutes like insulin, presumably due to their insignificant absorption from these upper airways (18). This model (comprised of differential equations and initial conditions; 10) was used to provide best estimates for the rate constants by subjecting the unweighted data sets for mean % of each administered dose (insulin or lispro) absorbed into perfusate vs. time following instillation (i.e., Fig. 5) to nonlinear least-mean-square regression analysis (Scientist™ for Windows; MicroMath Research, St. Louis, MO). Notably however, curve-fitting the cumulative absorption profiles to this model was incapable of deriving separate values for k_{mc} and k_{me}; thus, k_{mc} and k_{me} were combined and estimated as a single rate constant for "non-absorptive loss" (k_{nal}) from the PL region (Fig. 1). The data fits were assessed using "goodness-of-fit" statistics (Scientist™'s calculated Model Selection Criterion, MSC, and coefficient of determination, COD) alongside reviews of the final parameter estimates, their standard deviations and a visual inspection of all residuals.

RESULTS AND DISCUSSION

Hexamer Content (%Hex) in Insulin and Lispro Solutions

Figure 2 shows %Hex for Ins-Zn and Lispro-Zn at various concentrations (0.025–1.0 mg/ml) in 50 mM PBS at pH 7.4 or 5 mM PBS at pH 3.0, determined by QCUF-ZTT. Regardless of buffer concentration and pH, %Hex increased, as concentration increased within the range of 0.025–1.0 mg/ml. At concentrations ≥0.5 mg/ml, the values of %Hex for insulin and lispro in 50 mM PBS at pH 7.4 ($\mu = 0.28$ M) were essentially equivalent and by 1.0 mg/ml, approached 100%. In contrast, at concentrations <0.5 mg/ml, both polypeptides dissociated with Lispro-Zn showing greatest dissociation at a given concentration, due to the amino acid switch that causes reduced dimer formation (4,5,19). It was only under conditions of acidic pH and lower ionic strength ($\mu = 0.16$ M) that Ins-Zn exhibited increased dissociation at concentrations of 0.1–1.0 mg/ml (<12%; Fig. 2), as similarly reported in the literature (20). Overall, the insulin and lispro solutions prepared for the use in the IPRL as a dosing solution showed %Hex ranging from 3.3 to 94.4%.

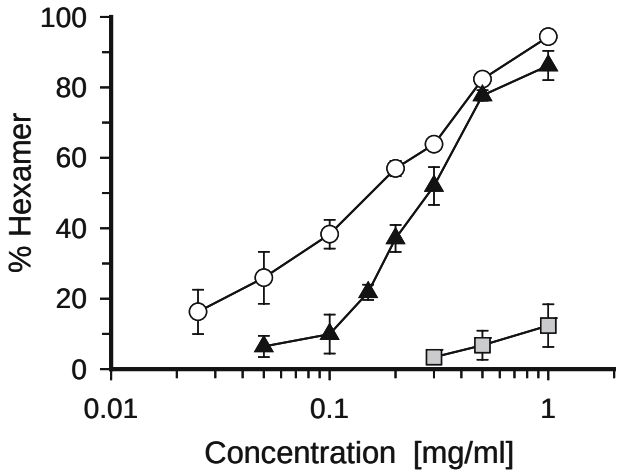

Fig. 2. Semi-logarithmic plots of mean %hexamer (%Hex; Eq. 2) as a function of human Ins-Zn or Lispro-Zn concentration in phosphate-buffered saline (PBS) at different pH, as determined by QCUF-ZTT. Error bars are standard errors (SE) from $n = 3$–12. Key: (○) Ins-Zn in 50 mM PBS at pH 7.4; (▲) Lispro-Zn in 50 mM PBS at pH 7.4; (□) Ins-Zn in 5 mM PBS at pH 3.0.

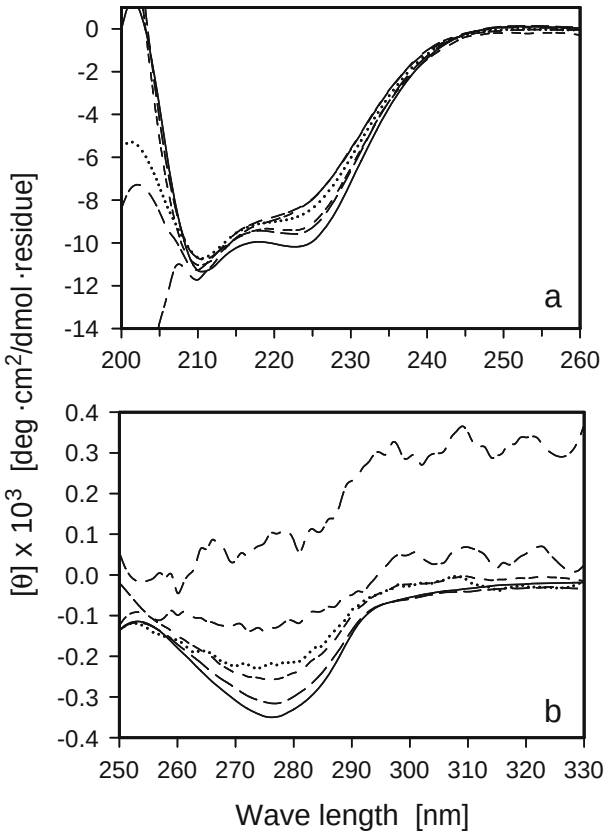

Fig. 3. (**a**) Far and (**b**) near UV CD spectra of human Ins-Zn at concentrations of 0.025, 0.05, 0.1, 0.2, 0.5 and 1.0 mg/ml in 50 mM PBS at pH 7.4. Increasing concentrations resulted in progressive depression of the values for mean residue molar ellipticity, [θ], and related spectra. Each spectrum was the average of three determinations; they were quite reproducible with ≤1.0% of relative standard deviation.

QCUF–ZTT results (Fig. 2) were consistent with the semi-quantitative data from far and near UV CD spectra. Far (200–260 nm) and near UV (250–330 nm) CD spectra of Ins–Zn at various concentrations (0.025–1.0 mg/ml) in 50 mM PBS at pH 7.4 are shown in Fig. 3; these were quite consistent with those reported previously (20–23). In Fig. 3a, two minima of [θ] were observed at 210 and 225 nm in the far UV spectra. With increasing insulin concentration, the negative intensity of $[\theta]_{210}$ changed slightly, but that of $[\theta]_{225}$ strengthened significantly. It has been suggested that $[\theta]_{210}$ primarily arises from α-helixes formed by the amino acid residues between insulin's B10–19, A2–6 and A13–19 residues, whereas $[\theta]_{225}$ reflects an antiparallel β-sheet structure formed as a result of insulin's dimerization (20–23). Thus, a decrease in the ratio, $[\theta]_{210}/[\theta]_{225}$, with increasing concentration is believed to reflect insulin's self-association to form dimers and hexamers (20–23). Indeed, as shown in Fig. 4, the values of $[\theta]_{210}/[\theta]_{225}$ decreased with increasing insulin concentration from 0.025 to 1.0 mg/ml and correspondingly, the increase in %Hex determined by QCUF–ZTT (Fig. 2). The near UV CD spectra shown in Fig. 3b possessed a single minimum at 275 nm ($[\theta]_{275}$) whose negative intensity also increased with increasing concentration from 0.025 to 1.0 mg/ml. This minimum $[\theta]_{275}$ is believed to result from rotatory restriction of insulin's aromatic side-chains (i.e., phenylalanine and tyrosine) due to self-association and hence, its negative intensity should also increase with increasing hexamer formation (20–23). Taken together, this semi-quantitative approach using far and near UV CD spectra is summarized in Fig. 4 as a function of Ins-Zn concentration. The data suggested a transition from non-associated monomers and dimers toward zinc bound hexamers over the concentration range studied in 50 mM PBS at pH 7.4, consistent with the results obtained from QCUF-ZTT (Fig. 2) for these dosing solutions.

Lung Disposition Kinetics of Insulin and Lispro and Hexameric Self-association

Figure 5a shows mean (±SE, $n = 4$) % of insulin dose transferred to perfusate of the IPRL vs. time following 0.1 ml doses of Ins-Zn solutions at various concentrations (0.05–1.0 mg/ml in 50 mM PBS at pH 7.4). Although apparently mono-phasic and first-order with ≈20 min half-lives ($t_{1/2}$), each of the absorption profiles appeared to approach different asymptotes; absorption at 60 min following instillation ranged from 2.7 to 7.6%. Once insulin concentrations became ≥0.3 mg/ml, profiles were statistically indistinguishable; the profiles at 0.05 and 0.1 mg/ml were significantly different from those at 0.3, 0.5 and 1.0 mg/ml ($p < 0.05$, ANOVA). Overall however, as Ins−Zn concentration in the dosing solution increased, the rate and extent of absorption decreased, thereby suggesting that dose- and/or concentration-dependent mechanisms somehow controlled insulin disposition kinetics in the IPRL.

Figure 5b shows a comparison of the absorption profiles for Ins-Zn and Lispro-Zn after dosing at the broad concentration extremes described above, 1.0 and 0.1 mg/ml in 50 mM PBS at pH 7.4. At 1.0 mg/ml where both polypeptides had been shown to exist as hexamers (Fig. 2), insulin and lispro displayed statistically indistinguishable absorption profiles ($p > 0.05$, ANOVA), with only 2.5% of each dose absorbed for 60 min. In contrast, lung absorption of lispro at 0.1 mg/ml (%Hex = 9.7%; Fig. 2) was faster and more extensive than that of insulin at the same concentration (%Hex = 38.3%; Fig. 2), showing 7.9% absorption at 60 min; these profiles were significantly different ($p < 0.05$, ANOVA). Kinetic analysis yielded $k_a = 0.22 \pm 0.05$ and $k_{nal} = 2.48 \pm 0.76$ h^{-1} for lispro at this 0.1 mg/ml dose, while insulin at the same concentration produced values of 0.14 ± 0.02 and 1.62 ± 0.30 h^{-1},

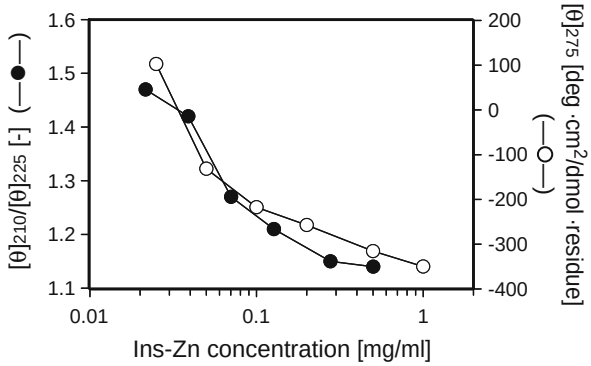

Fig. 4. Ratios of mean residue molar ellipticity, [θ], at 210 and 225 nm ($[\theta]_{210}/[\theta]_{225}$) and [$\theta$] values at 275 nm ($[\theta]_{275}$) for human Ins-Zn at various concentrations in 50 mM PBS at pH 7.4. Values were derived from the averaged CD spectra with ≤1.0% of relative standard deviation, as shown in Fig. 3.

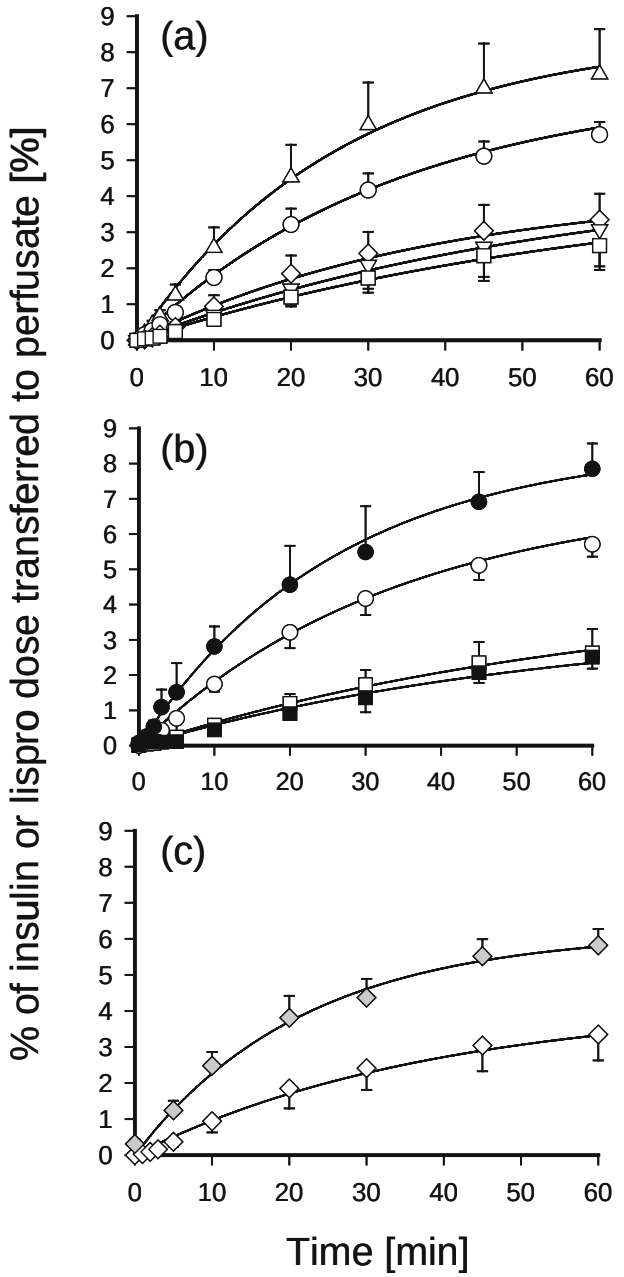

Fig. 5. Mean % of administered dose of immunoreactive insulin or lispro absorbed from the airways of the IPRL into perfusate vs. time following 0.1 ml forced solution instillations of human Ins-Zn or Lispro-Zn at various concentrations in PBS. Error bars are standard errors (SE; n = 4). Each of the solid curves is the result of curve fitting to the model shown in Fig. 1 using the best parameter estimates for the rate constants, k_a and k_{nal}. Panel: (**a**) Effect of Ins-Zn concentration. Key: (△) 0.05, (○) 0.1, (◇) 0.3, (▽) 0.5 and (□) 1.0 mg/ml in 50 mM PBS at pH 7.4; (**b**) Comparison between Ins-Zn and Lispro-Zn in 50 mM PBS at pH 7.4. Key: (○) Ins-Zn and (●) Lispro-Zn at 0.1 mg/ml and (□) Ins-Zn and (■) Lispro-Zn at 1.0 mg/ml; (**c**) Effect of solution pH and ionic strength. Key: (◇) Ins-Zn at 0.3 mg/ml in 50 mM PBS at pH 7.4 (μ = 0.28 M) and (◈) Ins-Zn at 0.3 mg/ml in 5 mM PBS at pH 3.0 (μ = 0.16 M). Statistical comparisons of these profiles are described in RESULTS AND DISCUSSION.

respectively. These observations of faster and more extensive absorption of lispro support the patent claim in this area (9) with the proviso that doses and formulations must create reduced association and lower values for %Hex in the airways.

Likewise, in Fig. 5c, Ins-Zn instillation at 0.3 mg/ml in 5 mM PBS at pH 3.0 (%Hex = 3.4%; Fig. 2) produced faster and greater absorption in the IPRL (apparent $t_{1/2} \approx 13$ min; 5.8% absorption at 60 min) than that from 50 mM PBS at pH 7.4 (%Hex = 63.8%; Fig. 2; $t_{1/2} \sim 18$ min; 3.4% absorption at 60 min); the profiles were significantly different ($p < 0.05$, ANOVA). The values for $k_a = 0.19 \pm 0.06$ and $k_{nal} = 3.55 \pm 1.06$ h^{-1} were obtained for 5 mM PBS at pH 3.0, while at pH 7.4, these became 0.07 ± 0.01 and 1.44 ± 0.44 h^{-1}, respectively. Whereas dosing solution pH could certainly play a part in this effect, the rate constants derived from the data at pH 3.0 fell on the general curves shown in Fig. 6, supporting earlier speculations (24) that the predominant kinetic determinant of pulmonary insulin kinetics could be the degree of association.

The solid curves in Fig. 5 are generated from the kinetic model shown in Fig. 1 using the best parameter estimates for k_a and k_{nal} via nonlinear least-mean-square regression analysis. Each of the curve-fits was excellent with MSC ≥ 4.67 and COD ≥ 0.994. Overall, the rate constants for absorption (k_a) and non-absorptive loss (k_{nal}) for Ins-Zn and Lispro-Zn ranged 0.03–0.22 and 0.90–3.55 h^{-1},

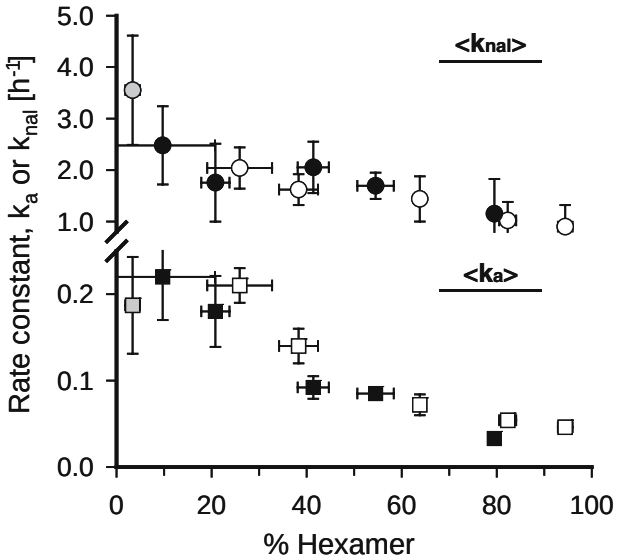

Fig. 6. Best parameter estimates of the rate constants for lung absorption, (□,■,▣) k_a, and non-absorptive loss, (○,●,◍) k_{nal}, for insulin and lispro as a function of mean %hexamer content (%Hex) in the dosing solutions. The rate constants were derived by curve-fitting the IPRL profiles (Fig. 5) to the model shown in Fig. 1, while the values for %Hex were determined by QCUF-ZTT shown in Fig. 2. Error bars in both the *X*- and the *Y*-axis are 95% confidence intervals (95%CI). Key: (□, ○) Ins-Zn in 50 mM PBS at pH 7.4; (■,●) Lispro-Zn in 50 mM PBS at pH 7.4; (▣, ◍) Ins-Zn in 5 mM PBS at pH 3.0. Notably, at %Hex ≥ 50%, the values for k_{nal} appear to approach the rate constant for mucociliary clearance (k_{mc}), 1.32 h^{-1}, determined previously in this IPRL (18).

respectively; these alongside values for the 95%CI are shown in Fig. 6. Values for k_a were clearly much smaller than those for k_{nal}, indicating that lung absorption of insulin and lispro was the slowest process overall and that this determined the kinetics of absorption in the IPRL. Because the values of k_a and k_{nal} decreased with increasing values for %Hex, each of the best estimates was plotted in Fig. 6 as a function of %Hex in the initial dosing solutions. Regardless of whether Ins-Zn or Lispro-Zn was administered or whether other conditions such as pH were changed, the rate constants appeared to depend only on %Hex, the magnitude of hexameric association in the dosing solution. In this sense, it became clear that insulin type, concentration, and buffer conditions in the dosing solution were secondary factors defining %Hex. As %Hex decreased, values for both k_a and k_{nal} increased (Fig. 6), suggesting that the kinetics of lung absorption and non-absorptive loss, the latter comprised of metabolism and mucociliary clearance (10), favored the dissociated forms of insulin. While logical with respect to the values for k_a, since smaller molecules are known to exhibit faster absorption (10), it was curious that, once %Hex ≥ 50%, the rate and extent of insulin absorption was essentially unaffected; in fact, both k_a and k_{nal} values became almost constant (Fig. 6). Notably, the values for k_{nal} at %Hex ≥ 50% approached those for the average rate constant for mucociliary clearance reported previously in this IPRL (k_{mc} = 1.32 h^{-1}; 18). It is likely, therefore, that insulin hexamers were not kinetically favorable subject to rapid metabolic degradation in the rat lung, unlike the dissociated forms, which exhibited k_{nal} values > 1.32 h^{-1} (Fig. 6). This observation was consistent with Liu *et al.* (25), in which *in vitro* metabolic degradation was slower for dissociated forms of insulin, compared to the associated (hexameric) counterparts. The fact that absorption continued, even as %Hex approached 100% (k_a remained finite and > 0.02 h^{-1}; Fig. 6), implied either that a finite proportion of monomeric insulin was formed in the airways to drive the absorption process, or that slow hexamer absorption could occur without dissociation or both.

It should be noted that counterarguments exist in the literature (26,27) with respect to the effect of self-association upon pulmonary insulin kinetics. Liu *et al.* (26) reported that intratracheal instillation (0.1 ml) of "hexameric" zinc and "dimeric" sodium insulin at 40 IU/ml (≈1.4 mg/ml) resulted in no significant difference in their blood glucose reduction responses in rats; unfortunately, the association states of neither form of insulin was determined, leaving the finding inconclusive. Indeed, Birnbaum *et al.* (4) reported ≥50% of hexamer formation for zinc-free (e.g., sodium) insulin at an equivalent concentration ≈1.4 mg/ml (40 IU/ml), making it likely that Liu's results were dominated by the study of hexamer-rich compositions. Most recently, insulin and lispro were tested in rats, prepared from Humulin® and Humalog®, respectively by Hussain and Ahsan (27). Their *in vivo* plasma concentration profiles following 0.1 ml microspray administration at doses of 0.6–10 IU/kg (0.05–0.8 mg/ml solutions) could not be distinguished statistically, again implying that self-association was not an important determinant of pulmonary insulin kinetics. In that case, in addition to the lack of reported association state data, the authors' argument is apparently hampered by the presence of formulation excipients (*m*-cresol and glycerol) and overly large reported plasma concentrations, when compared to those from pure insulin (without excipients) at equivalent doses (28).

Lung Disposition Kinetics of Insulin in STZ-induced Experimental Diabetes

A rat model of STZ-induced experimental diabetes has been commonly used in diabetic research (12). The model primarily features Type 1 diabetes due to pancreatic β cell necrosis, while also resembling certain aspects of Type 2 diabetes in the long-term (12). In lung, several physiological, biochemical and structural changes have been demonstrated in this model (29–32). It has been shown that rat airspaces can be diminished in size, the alveolar epithelium may collapse, and the capillary endothelium contains numerous plasmalemmal vesicles like cavaolae (29,30). The model has also been associated with decreased lung surfactant and increased certain enzyme activities (e.g., angiotensin converting enzyme) within the airways (31,32). Clearly, it was important to determine whether such pathological changes could alter the lung disposition of pulmonary insulin. Following STZ-injections and glycemic analysis in accord with Chandrashekar's model (15), the blood glucose of the experimental diabetic group of animals reached 274 ± 20 mg/dl (mean ± SD, n = 5) at 2 weeks. This value was considered abnormal and significantly higher than 98 ± 20 mg/dl observed in the matched sham-control (Table I). Ins-Zn at 0.1 mg/ml in 50 mM PBS at pH 7.4 (0.1 ml; %Hex = 38.3%; Fig. 2) was administered into the IPRL preparations from both groups of animals, and their absorption profiles compared and analyzed, as described above. Table I summarizes the rate constants for k_a and k_{nal} derived via curve-fitting the data from the absorption profiles of the STZ-induced experimental diabetic and matched sham-control animals, alongside the "goodness-of-fit" parameters. There was no significant difference between the profiles from these two groups of IPRL preparations (ANOVA, $p > 0.05$; the profiles not shown), and the derived rate constants for k_a and k_{nal} were unchanged by this experimental disease state. The values for k_a and k_{nal} were also consistent with those obtained from the normal untreated animals described above (Figs. 5a and 6).

%Hex in Airway Fluids: Rats and Humans

One final question should be posed, given the apparent dependence of k_a and k_{nal} on %Hex in the dosing solutions reported here, 'how representative were these values for %Hex in each dosing solution of the same variable at the site of these kinetic events, i.e., in the lung lining fluid (LLF) of the IPRL.' This exercise is important, since it is not possible to determine the magnitude and kinetics of insulin's self-association *in situ* in the lung, any more than it was possible for subcutaneous insulin and lispro at an injection site (2–5). In this study, the dosing volume (0.1 ml) was chosen so that it was approximately equivalent to the normal volume of LLF in this IPRL (≈0.1 ml; 33). It has been shown previously that LLF volume is well-maintained by Na^+-derived, osmotic pressure-driven airway-to-capillary fluid transport mechanisms, with a rapid rate of re-equilibration, ≈12 μl/min in response to the slight LLF volume changes caused by solution instillation (33). As a result, in theory, LLF volume should be restored to

its normal value (≈0.1 ml) within 10 min following 0.1 ml instillation employed in this study. This should mean that %Hex in each dosing solution would be a close approximation of that observed in the LLF of this IPRL ≈ 10 min post-instillation, offering a reasonable rationale for the correlation shown in Fig. 6. This rather complex argument was necessary because of our inability to quantify %Hex directly, on the lung surface. Unless there are other complications, our logic implies that the horizontal axis of Fig. 6, %Hex in the dosing solutions, is a close approximation of %Hex in the airways shortly after administration. This indirect argument is similar to that used to discuss lispro pharmacokinetics following subcutaneous injection (5).

Apparently, the situation in these rat lungs differs from that in human lungs for inhaled insulin, because of the latter's much larger LLF volume (≈10 ml). Inhalation of powder or liquid formulations of insulin, such as Exubera® or AERx iDMS®, respectively, by humans should result in dissolution and/or dilution in LLF. With the assumption that clinically effective insulin doses of 0.6–1.8 IU/kg (34) are uniformly distributed to the entire LLF of the human lung (i.e., 10 ml), 0.16–0.47 mg/ml insulin concentrations are possible in LLF. If so, values for %Hex in LLF are likely to exceed 50%, based on the QCUF–ZTT data shown in Fig. 2. Accordingly, if the IPRL data (Figs. 5 and 6) are predictive of the human situation, the lung disposition kinetics in humans at this dose range (0.6–1.8 IU/kg) should become mostly dose-independent by virtue of hexamer-rich (≥50%) compositions in LLF. Such an observation is consistent with our earlier meta-analysis for lung disposition kinetics of inhaled insulin in humans (34) where effectively constant kinetic parameters for lung absorption and disposition across this range of inhaled doses were observed. In contrast, and as implied from Fig. 5b, inhalation of lispro at a low dose of 0.3 IU/kg in humans showed faster absorption than regular insulin (9). This can be attributed to a much lower 0.08 mg/ml of lispro or only ≈7% of %Hex, in the LLF. Thus, faster lung absorption may become feasible even in humans inhaling "monomeric" insulin analogues like lispro or aspart, provided reduced doses are possible.

CONCLUSION

The present study has shown that lung disposition kinetics of pulmonary insulin and lispro in the IPRL depend on the magnitude of hexameric association (%Hex) in the dosing solution, a situation similar to subcutaneous injection. Irrespective of insulin type or concentration, solution pH or ionic strength or normal or experimental diabetic states, excellent correlations were observed between each of the kinetic parameters for lung disposition in the IPRL, k_a and k_{nal}, and %Hex determined by the QCUF-ZTT method (Fig. 6 and Table I). The values for k_a (absorption) decreased ($0.22 \rightarrow 0.05\ h^{-1}$) with increasing %Hex (Fig. 6). Values for k_{nal} (comprising mucociliary clearance and metabolism) also decreased ($3.84 \rightarrow 0.90\ h^{-1}$) with increasing %Hex, although, at %Hex ≥ 50%, values approached that of the rate constant for mucociliary clearance (Fig. 6). This %Hex-dependent correlation for k_a and k_{nal} indicated a kinetic preference of lung absorption and metabolism for insulin dimers and monomers over hexameric counterparts. This appears to explain some features of inhaled insulin pharmacokinetics in humans. At clinically effective inhaled doses (0.6–1.8 IU/kg), hexamer-rich (%Hex ≥ 50%) compositions are likely to be formed in lung lining fluids (LLF) following inhalation, thereby resulting in mostly dose-independent pharmacokinetics. Even so, faster and increased absorption may become feasible using "monomeric" insulin analogues like lispro and aspart, especially if inhaled doses can be reduced significantly.

ACKNOWLEDGMENTS

The authors are grateful to Eli Lilly and Company for their gift of lispro-zinc (Lispro-Zn), and to Verne G. Schirch, Ph.D. (Department of Biochemistry, VCU) for the use and assistance with CD spectrometry. The Medical College of Virginia Foundation and VCU's A.D. Williams Research Funds (MS) supported this research. YP acknowledges VCU School of Pharmacy financial support during her graduate study.

REFERENCES

1. J. Brange. *Galenics of insulin*, Springer, Berlin, 1987.
2. M. R. DeFelippis, R. E. Chance, and B. H. Frank. Insulin self-association and the relationship to pharmacokinetics and pharmacodynamics. *Crit. Rev. Ther. Drug Carr. Syst.* **18**:201–264 (2001).
3. S. Kang, J. Brange, A. Burch, A. Volund, and D. R. Owens. Subcutaneous insulin absorption explained by insulin's physicochemical properties. *Diabetes Care* **14**:942–948 (1991).
4. D. T. Birnbaum, M. A. Kilcomons, M. R. DeFelippis, and J. M. Beals. Assembly and dissociation of human insulin and $Lys^{B28}Pro^{B29}$-insulin hexamers: a comparison study. *Pharm. Res.* **14**:25–36 (1997).
5. Z. Vajo and W. C. Duckworth. Genetically engineered insulin analogs: diabetes in the new millennium. *Pharmacol. Rev.* **52**:1–9 (2000).
6. S. J. Farr and G. Taylor. Insulin inhalation: its potential as a nonparenteral method of administration. In A. L. Adjei and P. K. Gupta (eds.), *Inhalation Delivery of Therapeutic Peptides and Proteins*, Marcel Dekker, New York, 1997, pp. 371–387.
7. J. S. Patton, J. G. Bukar, and M. A. Eldon. Clinical pharmacokinetics and pharmacodynamics of inhaled insulin. *Clin. Pharmacokinet.* **43**:781–801 (2004).
8. K. Rave, S. Bott, L. Heinemann, S. Sha, R. H. Becker, S. A. Willavize, and T. Heise. Time-action profile of inhaled insulin in comparison with subcutaneously injected insulin lispro and regular human insulin. *Diabetes Care* **28**:1077–1082 (2005).
9. I. Gonda, R. M. Rubsamen, and S. J. Farr. Method of use of monomeric insulin as a means for improving the reproducibility of inhaled insulin. *United States Patent*, US 6250298 (Jun 26, 2001).
10. Y. Pang, M. Sakagami, and P. R. Byron. The pharmacokinetics of pulmonary insulin in the *in vitro* isolated perfused rat lung: implications of metabolism and regional deposition. *Eur. J. Pharm. Sci.* **25**:369–378 (2005).
11. R. A. Roth. Flow dependence of norepinephrine extraction by isolated perfused rat lungs. *Am. J. Physiol.* **242**:H844–H848 (1982).
12. B. Rodrigues, P. Poucheret, M. L. Battell, and J. H. McNeill. Streptozotocin-induced diabetes: induction, mechanism(s), and dose dependency. In J. H. McNeill (ed.), *Experimental Models of Diabetes*, CRC Press, Florida, 2000, pp. 3–17.
13. S. Rahuel-Clermont, C. A. French, N. C. Kaarsholm, M. F. Dunn, and C. I. Chou. Mechanisms of stabilization of the insulin hexamer through allosteric ligand interactions. *Biochemistry* **36**:5837–5845 (1997).
14. R. H. Holyer, C. D. Hubbard, S. F. A. Kettle, and R. G. Wilkins. The kinetics of replacement reactions of complexes of the transition metals with 2,2′,2″-terpyridine. *Inorg. Chem.* **5**:622–625 (1966).

15. V. Chandrashekar, R. W. Steger, A. Bartke, C. T. Fadden, and S. G. Kienast. Influence of diabetes on the gonadotropin response to the negative feedback effect of testosterone and hypothalamic neurotransmitter turnover in adult male rats. *Neuroendocrinology* **54**:30–35 (1991).
16. P. R. Byron and R. W. Niven. A novel method for drug administration to the airways of the isolated perfused rat lung. *J. Pharm. Sci.* **77**:693–695 (1988).
17. J. Z. Sun, P. R. Byron, and F. Rypacek. Solute absorption from the airways of the isolated rat lung. V. Charge effects on the absorption of copolymers of N(2-hydroxyethyl)-DL-aspartamide with DL-aspartic acid or dimethylaminopropyl-DL-aspartamide. *Pharm. Res.* **16**:1104–1108 (1999).
18. M. Sakagami, P. R. Byron, J. Venitz, and F. Rypacek. Solute disposition in the rat lung *in vivo* and *in vitro*: determining regional absorption kinetics in the presence of mucociliary escalator. *J. Pharm. Sci.* **91**:594–694 (2001).
19. D. N. Brems, L. A. Alter, M. J. Beckage,R. E. Chance, R. D. DiMarchi, L. K. Green, H. B. Long, A. H. Pekar, J. E. Shields, and B. H. Frank. Altering the association properties of insulin by amino acid replacement. *Protein Eng.* **5**:527–533 (1992).
20. G. D. Fasman. *Circular dichroism and the conformational analysis of biomolecules*, Plenum, New York, 1996.
21. Y. Pocker and S. B. Biswas. Conformational dynamics of insulin in solution. Circular dichroic studies. *Biochemistry* **19**:5043–5049 (1980).
22. K. Hinds, J. J. Koh, L. Jones, F. Liu, M. Baudys, and S. W. Kim. Synthesis and characterization of poly(ethylene glycol)-insulin conjugates. *Bioconjug. Chem.* **11**:195–201 (2000).
23. S. G. Melberg and W. C. Johnson. Changes in secondary structure follow the dissociation of human insulin hexamers: a circular dichroism study. *Proteins* **8**:280–286 (1990).
24. K. Okumura, S. Iwakawa, T. Yoshida, T. Seki, and F. Komada. Intratracheal delivery of insulin: absorption from solution and aerosol by rat lung. *Int. J. Pharm.* **88**:63–73 (1992).
25. F. Liu, D. O. Kildsig, and A. K. Mitra. Insulin aggregation in aqueous media and its effect on alpha-chymotrypsin-mediated proteolytic degradation. *Pharm. Res.* **8**:925–929 (1991).
26. F. Y. Liu, Z. Shao, D. O. Kildsig, and A. K. Mitra. Pulmonary delivery of free and liposomal insulin. *Pharm. Res.* **10**:228–232 (1993).
27. A. Hussain and F. Ahsan. State of insulin self-association does not affect its absorption from the pulmonary route. *Eur. J. Pharm. Sci.* **25**:289–298 (2005).
28. S. Suarez, L. Garcia-Contreras, D. Sarubbi, E. Flanders, D. O'Toole, J. Smart, and A. J. Hickey. Facilitation of pulmonary insulin absorption by H-MAP: pharmacokinetics and pharmacodynamics in rats. *Pharm. Res.* **18**:1677–1684 (2001).
29. D. Popov and M. Simionescu. Alterations of lung structure in experimental diabetes, and diabetes associated with hyperlipidaemia in hamsters. *Eur. Respir. J.* **10**:1850–1858 (1997).
30. M. Pascariu, M. Bendayan, and L. Ghitescu. Correlated endothelial caveolin overexpression and increased tanscytosis in experimental diabetes. *J. Histochem. Cytochem.* **52**:65–76 (2004).
31. K. Sugahara, K. Iyama, K. Sano, and T. Morioka. Overexpression of pulmonary surfactant apoprotein A mRNA in alveolar type II cells and nonciliated bronchiolar (Clara) epithelial cells in streptozotocin-induced diabetic rats demonstrated by in situ hybridization. *Am. J. Respir. Cell Mol. Biol.* **6**:307–314 (1992).
32. A. Erman, B. Chen-Gal, I. David, S. Giler, G. Boner, and D. J. van Dijk. Insulin treatment reduces the increased serum and lung angiotensin converting enzyme activity in streptozotocin-induced diabetic rats. *Scand. J. Clin. Lab. Invest.* **58**:81–87 (1998).
33. M. Sakagami and P. R. Byron. Osmotic effects on solute absorption from the airways: implication for solute-uncoupled alveolar fluid transport. *AAPSPharmSci* **3** (2001) http://www.aapspharmaceutica.com/search/abstract_view.asp?id=535&ct=01Abstracts.
34. M. Sakagami. Insulin disposition in the lung following oral inhalation in humans: a meta-analysis of its pharmacokinetics. *Clin. Pharmacokinet.* **43**:539–552 (2004).